Phase Diagram and Scaling of Granular Materials under Horizontal Vibrations

Gerald H. Ristow
Fachbereich Physik, Philipps-Universität, Renthof 6, 35032 Marburg, Germany

Gunther Straßburger and Ingo Rehberg
Otto-von-Guericke Universität, Institut für Experimentelle Physik, Postfach 4120, 39016 Magdeburg, Germany
(Received 13 September 1996; revised manuscript received 16 April 1997)

Horizontal vibration of a granular material is studied experimentally and by means of molecular dynamics simulations. We focus on the transition from a more solidlike behavior of the granulate, which is obtained at small driving velocities, to a more fluidlike behavior for higher velocities. We present two different order parameters suitable to characterize the transition, namely the granular temperature and the pair distribution function. When using different frequencies f and amplitudes A_0 of the vibration, we find that the transition point from the solid to the fluid phase scales with $A_0 f^2$, whereas the granular temperature scales as $(A_0 f)^{1.66}$. [S0031-9007(97)03770-8]

PACS numbers: 46.10.+z, 47.50.+d, 64.60.Cn, 81.05.Rm

Even though we are surrounded by granular materials and they are widely used in industrial applications, their physical properties are far from being fully understood (for a recent review, see [1] and references cited therein). One of the most fascinating peculiarities of granular matter is their transition from a solidlike behavior to a fluidlike behavior (fluidization) [2], which appears when increasing the strength of external shear or the amplitude of vibration [3]. In most experiments, this transition seems fairly obvious just by visual inspection of the granulate, although a precise determination is not possible: Individual grains do move both below and above the fluidization point. An objective order parameter suitable for measuring this fascinating transition from solidlike to fluidlike behavior is missing so far. We propose two such order parameters here, one being based on the so-called granular temperature, the other one extracted from the pair distribution function. By using these order parameters, we are able to identify the scaling of the fluidization point and find that it scales with the *acceleration* of the vibration. This behavior was also observed for the threshold of the free surface instability [4] and the spontaneous heaping instability [5] in sand piles undergoing vertical vibrations. On the other hand, all data points lie on one universal curve when rescaled with the *velocity* of the vibration which is reminiscent of the scaling for the height of the center of mass of a granulate under vertical vibration [6,7] or the scaling of the granular temperature in that experiment [6,8].

The experimental apparatus allows for a horizontal vibration of granulate and is similar to the one described in Ref. [9]. The shaker is a commercial one (Bühler SM 25 DIGI), where the mechanics have been rebuilt in order to give a sinusoidal vibration. The available amplitude is in the range of 0–21 mm, and the frequency ranges from 0.9–4.3 Hz. For amplitudes above 21 mm or frequencies above 4 Hz an *X*-*Y* plotter is used. We use a channel of 100 mm length in the direction of the vibration, 0.6 mm width, and 20 mm height. The container is filled with granular material consisting of commercially available glass ballotonies. According to a microscopic observation, the shape of these beads is almost spherical. We have developed a procedure to get rid of the particles which deviate considerably from this shape, by making use of the different rolling behavior of spheres and nonspherical particles down an inclined plane. The diameter of the spheres ranges between 0.52 and 0.6 mm. The lower boundary is determined by a sieving procedure, and the upper boundary is determined both by a sieving procedure and by the channel width. The channel is filled with a monolayer of spheres, and the height of the granulate is 3–5 particles, i.e., we use about 700 particles. No attempt has been made to count this number exactly, however, because the physics of interest in this article, namely the solid-fluid transition, seems to be fairly independent of the exact number. The particle motion is measured in the comoving frame by means of a Sony XC-77CE CCD camera. The image is pixelsynchronically digitized by a BFT-AT/20 framegrabber.

In searching for an order parameter to characterize the solid-fluid transition at a sufficiently large amplitude of the horizontal vibration, the camera observes the central 40 mm of the channel from the side, i.e., perpendicular to the direction of the oscillation. Thirty-two snapshots are digitized with a sampling rate of 25 Hz. In order to overcome the difficulties of inhomogeneous illumination, we obtain a binary image by giving pixels associated with the background a value of zero and pixels associated with a particle the value of 1. We then characterize fluidization by comparing consecutive images. To do so, we subtract consecutive binary images and take the mean square of the resulting difference. The resulting number is called *pixel change*. In order to obtain a temporal mean value

over about one period of the driving, we take the mean value of about 7 (depending on the driving frequency) such pixel changes. The resulting number is plotted in Fig. 1 as a function of the vibration frequency of the apparatus, for a fixed amplitude of 20 mm. For low frequencies, the pixel change is zero, indicating that the particles do not move. Above 2.5 Hz the value increases slightly, which we attribute to the motion of at least a small fraction of particles. The dramatic increase of the pixel change around 3 Hz serves to define the transition to the fluidized phase. Open circles are drawn when increasing the frequency between the measurements and solid circles represent data taken after decreasing the driving frequency. By comparison, one can easily resolve some hysteresis for this transition. We determine the critical frequency f_c for the onset of fluidization by fitting a straight line to the supercritical values. Its intersection with the frequency axis yields $f_c = 2.9$ Hz. The onset of the motion of individual particles, denoted f_0, is clearly below this frequency (see Fig. 6 below).

In order to study granular materials using computer simulations in two dimensions, we represent each particle i by a sphere with radius d_i. Only contact forces during collisions are considered and particles are allowed to rotate. The forces acting on particle i during a collision with particle j are in the normal direction ($\hat{n}$)

$$F_{ij}^n = -k_n(d_i + d_j - \vec{r}_{ij}\hat{n}) - \gamma_n \vec{v}_{ij}\hat{n} \qquad (1)$$

and in the shear direction ($\hat{s}$)

$$F_{ij}^s = \mathrm{sgn}(\vec{v}_{ij}\hat{s}) \min(\gamma_s \vec{v}_{ij}\hat{s}, \mu|F_{ij}^n|) . \qquad (2)$$

Here $\vec{r}_{ij}$ stands for the vector joining both centers of mass and $\vec{v}_{ij}$ denotes the relative velocity of the two particles. For the details of the numerical model we refer the reader to a review article and references cited therein [10]. The four model parameters $(k_n, \gamma_n, \gamma_s, \mu)$ have the following physical interpretation: k_n is related to the material stiffness, γ_n to the energy loss during collisions (in experiments measured via the restitution coefficient), and the pair γ_s and μ controls the energy loss and static friction in the shear direction, e.g., via the surface roughness. Commonly, μ is referred to as the Coulomb friction coefficient. In our simulations we use a value of $\gamma_s = 1$ N s/m which was sufficiently high so that the shear forces were dependent on μ only and k_n was set to 10^6 N/m. The rest of the parameters were chosen from the detailed collision experiments using glass beads by Foerster *et al.* [11] as $\gamma_n = 5.75$ N s/m which corresponds to a restitution coefficient of 0.75 in the normal direction and values of $\mu = 0.1$ for particle-particle and $\mu_w = 0.13$ for particle-wall contacts. In our model, we dissipate energy in the shear direction as well characterized by a restitution coefficient of 0.75. The box length was 10.08 cm with periodic boundary conditions in the direction of shaking (x direction) and contained 343 particles in two layers. We use a polydisperse diameter distribution ranging uniformly from 0.52 to 0.60 mm which corresponds to the beads used in our experimental system.

To determine the fluidization point the situation is more transparent in the numerical simulations since the position and velocity informations of all particles are given at any time. Noting that the pixel changes in Fig. 1 correspond to particles that have moved in the laboratory frame, we took as a quantitative measure for the phase transition in the numerical system the granular temperature which is proportional to the velocity fluctuations, $T_g \equiv \frac{1}{N}\sum_{i=1}^{N} \frac{m_i}{2}(\vec{v}_i - \langle \vec{v} \rangle)^2$, where $\langle \vec{v} \rangle \equiv \frac{1}{N}\sum_{i=1}^{N} \vec{v}_i$. It is averaged over an integer number of full cycles of the external excitation frequency and shown in Fig. 2 as a function of frequency for the same amplitude as used in Fig. 1. The error bars are less than the symbol size. T_g is approximately zero for low frequencies and increases monotonically after a transition point which we estimate

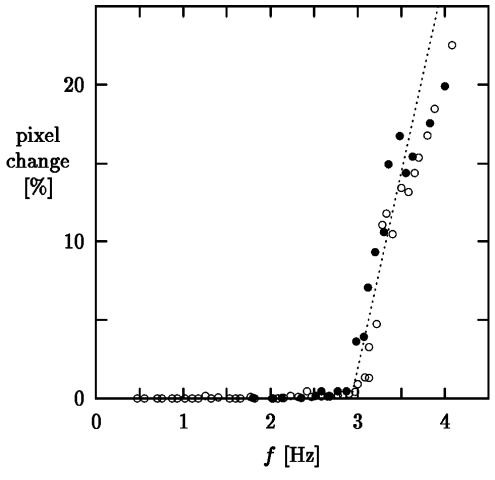

FIG. 1. Experimental system: relative pixel change as function of the external frequency for an amplitude of 2 cm; increasing frequency: ○, decreasing frequency: ●; the dotted line shows our linear fit to determine the critical point f_c.

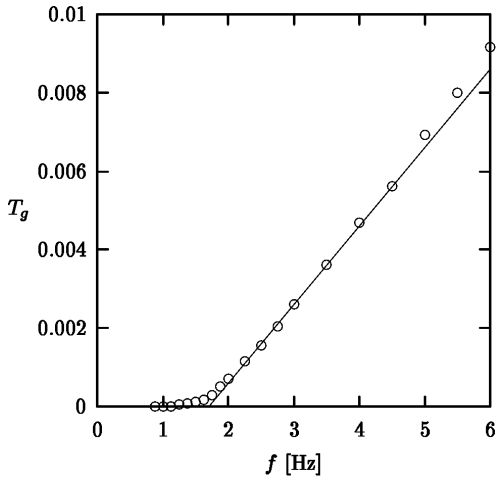

FIG. 2. Granular temperature for the numerical system as function of the external frequency for an amplitude of 2 cm.

in a similar procedure as described above as $f^* = 1.7 \pm 0.3$ Hz for $A_0 = 2$ cm. The experimental and numerical systems both show the same qualitative behavior with a well-defined transition point. Changing the restitution coefficient in normal direction in the numerical simulations did not change this transition point. On the other hand, changing the Coulomb friction coefficient μ has a dramatic effect. Setting it to zero lowers the transition point by 0.5 Hz and increasing it to 1 roughly increases the transition point by 1 Hz as well. We feel that the surface properties of our experimental system does lead to a higher value of μ than measured by Foerster *et al.* [11] which will explain the slight shift. Varying the length of the box size did not change the transition point.

An alternative measure for the transition point can be obtained by looking at the pair distribution function (PDF) defined as $G(r) \equiv \frac{V}{N^2} \langle \sum_i \sum_{j \neq i} \delta(|\vec{r} - \vec{r}_{ij}|) \rangle$ [12]. It measures the probability density to find a particle at a distance r from another particle and is normalized to one for a completely random configuration. Clear double peaks are seen around integer values of r/d ($d = 0.56$ mm denotes the average particle diameter) when the system is at rest or only slightly excited, as shown in Fig. 3(a) for $A_0 = 2$ cm and $f = 1.25$ Hz, which is due to the two-dimensional hexagonal packing. Since only two layers of particles are present in our numerical system, we do not distinguish between surface and bulk particles but include all particle pairs in the calculation of the PDF. For the histogram we used a box width of dr. The height of the peaks decreases with increasing r because we have a finite system and polydisperse particles. If the external excitation is increased, either by increasing the amplitude or the frequency, the height and the number of clearly visible peaks decreases drastically, as shown in Fig. 3(b) for $f = 4.25$ Hz. This technique was, e.g., successfully used to study the melting transition in plasma crystals [13]. In order to quantify the decay of spatial order, we look at the height of the PDF at $r = \sqrt{3}d$ and $r = 2d$, which corresponds to two peaks in the hexagonal packing. The latter corresponds to order within the same particle layer, whereas the first measures the order with respect to the neighboring layer. In an infinite solid phase, both peaks have the same height, whereas the peak around $r \approx \sqrt{3}d$ decreases more rapidly when the excitation is increased and fluidization sets in, see, e.g., Fig. 3(a). We propose as second order parameter the ratio of the heights of these peaks denoted by P_2/P_3. This is illustrated in Fig. 4 for a shaking amplitude of 2 cm. A qualitative change of the curve is seen around $f = 1.6$ Hz when the nearly constant ratio starts to decrease monotonically. This change corresponds to the transition point and its value, given by the intersection of the two straight lines in Fig. 4, is in perfect agreement with the one obtained using the granular temperature.

The increase with frequency of the kinetic energy or the granular temperature varies largely with excitation amplitude. But all curves collapse onto one universal curve when they are plotted as function of the dimensionless parameter $\Gamma \equiv A_0(2\pi f)^2/g$, where g denotes the gravitational constant and the granular temperature is rescaled with the maximum excitation velocity to the power of 1.66, which might be related to the 5/3 law discussed by Taguchi [14] and Ichiki and Hayakawa [15]. Here we use dimensionless quantities denoted by the superscript s using the average mass and diameter of a particle and also g, which is shown in Fig. 5 for three different shaking amplitudes. It is reminiscent of the scaling of the center of mass of a granulate under vertical vibration in two-dimensional simulations, where an exponent of 1.5 was found [7]. The error in our exponent is 0.05.

In order to find the correct scaling parameter for the horizontal shaking experiment, we look at a

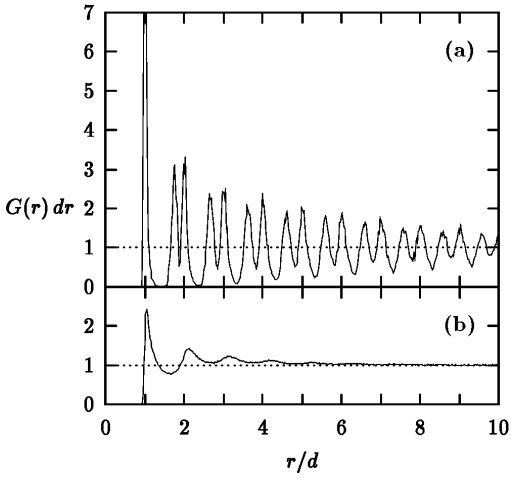

FIG. 3. Pair distribution function for the numerical system at a shaking amplitude of 2 cm (a) at low frequency of 1.25 Hz and (b) at high frequency of 4.25 Hz.

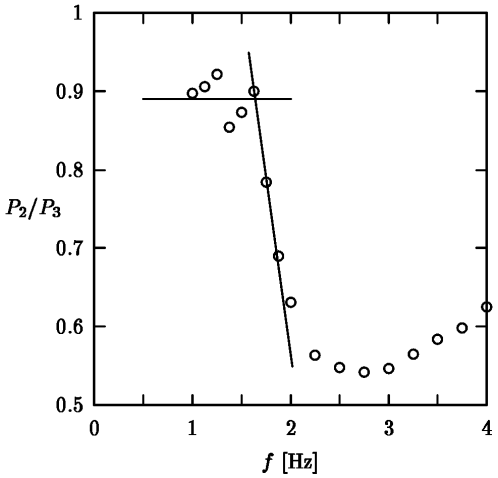

FIG. 4. Ratio of the second and third peak of the pair distribution function for the numerical system as function of the external frequency for an amplitude of 2 cm.

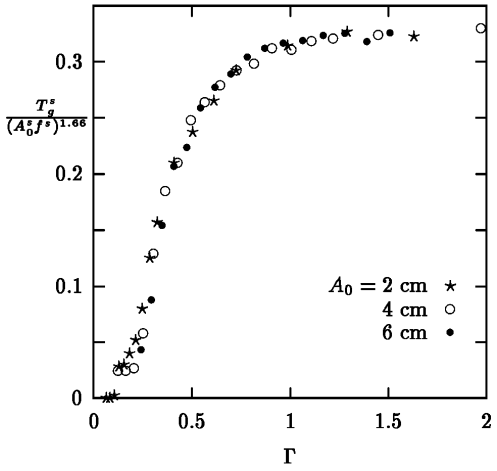

FIG. 5. Numerical simulations: rescaling of the granular temperature as function of $\Gamma \equiv A_0(2\pi f)^2/g$.

two-dimensional cross section of the system similar to the one used in the numerical simulation. Since the particles vary in diameter by only $\pm 7\%$, a nearly hexagonal packing is found when the vibrations are switched off, i.e., one cylinder in the upper layer rests on two cylinders from the next layer below. For an estimate of the solid-fluid transition, one can then calculate the critical acceleration where a single cylinder would begin to move within the valley formed by these two cylinders to be $a_c = g \tan 30°$. This yields a scaling of the critical frequency with the amplitude as follows: $f_c \sim \sqrt{g/A_0}$.

Figure 6 summarizes the results of the experimental, theoretical, and numerical estimates of the solid-fluid transition. In order to avoid the ambiguity caused by the rounded transition from a solidlike to a fluidlike state, we present the amount of the pixel using a gray scale. The transition from no movement to a 1% change corresponds to the transition denoted f_0 above. It seems to agree fairly well with the analytical argument and with the results of the molecular dynamics simulation. The experimentally determined solid-fluid transition, denoted f_c, is obtained at slightly larger values of the driving acceleration. The difference between theory and experiment might be due to the additional friction caused by the sidewalls in the experimental setup.

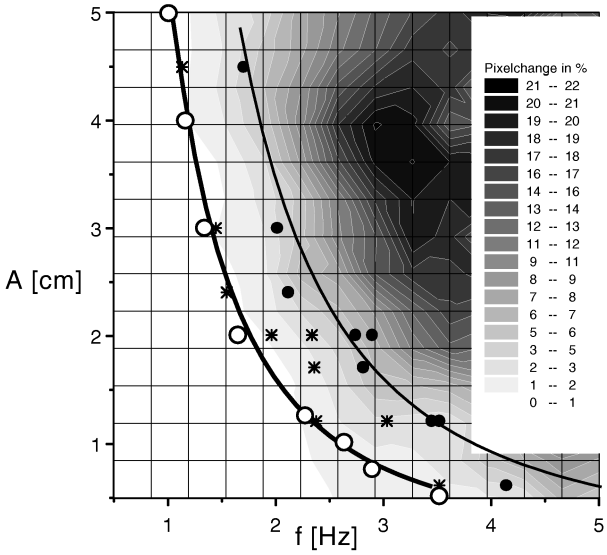

FIG. 6. Phase diagram for the solid-fluid transition: experimental points $*$ (f_0) and ● (f_c) with gray scale image of the pixel change (see legend); data from numerical simulations ○ with thick solid line as best fit. Thin solid line shows theoretical curve.

In summary, we have provided order parameters capable of characterizing the fluidization point in a granulate. The transition point scales with the acceleration of the driving vibration. Slightly above the fluidization point, pattern formation has been reported to occur in horizontally vibrated sand layers [9]. A characterization of this instability and its scaling behavior is currently in progress.

We thank A. Betat, R. Clos, S. Grossmann, S. Linz, and M.A. Scherer for enlightening discussions. The experiments are supported by Deutsche Forschungsgemeinschaft through Re 588/11-1 and the numerical simulation through Ri 826/1-1.

[1] H. M. Jaeger, S. R. Nagel, and R. P. Behringer, Phys. Today **4**, 32 (1996).
[2] S. E. Esipov and T. Pöschel, J. Stat. Phys. **86**, 1385 (1997).
[3] E. Clément and J. Rajchenbach, Europhys. Lett. **16**, 133 (1991); J. A. C. Gallas, H. J. Herrmann, and S. Sokołowski, Physica (Amsterdam) **A189**, 437 (1992).
[4] P. Evesque and J. Rajchenbach, Phys. Rev. Lett. **62**, 44 (1989).
[5] E. Clément, J. Duran, and J. Rajchenbach, Phys. Rev. Lett. **69**, 1189 (1992).
[6] S. Warr, J. M. Huntley, and G. T. H. Jacques, Phys. Rev. E **52**, 5583 (1995).
[7] S. Luding, H. J. Herrmann, and A. Blumen, Phys. Rev. E **50**, 3100 (1994).
[8] J. Lee, Physica (Amsterdam) **A219**, 305 (1995).
[9] G. Straßburger, A. Betat, M. A. Scherer, and I. Rehberg, in *Traffic and Granular Flow*, edited by D. E. Wolf, M. Schreckenberg, and A. Bachem (World Scientific, Singapore, 1996).
[10] G. H. Ristow, in *Annual Reviews of Computational Physics I*, edited by D. Stauffer (World Scientific, Singapore, 1994), pp. 275-308.
[11] S. F. Foerster, M. Y. Louge, H. Chang, and K. Allia, Phys. Fluids **6**, 1108 (1994).
[12] M. P. Allen and D. J. Tildesley, *Computer Simulation of Liquids* (Clarendon Press, Oxford, 1990).
[13] A. Melzer, A. Homann, and A. Piel, Phys. Rev. E **53**, 2757 (1996).
[14] Y-h. Taguchi, Europhys. Lett. **24**, 203 (1993).
[15] K. Ichiki and H. Hayakawa, Phys. Rev. E **52**, 658 (1995).